# Long-distance placement of substrate RNA by H/ACA proteins

BO LIANG,[1] ELLIOT J. KAHEN,[2] KATE CALVIN,[1] JING ZHOU,[2] MARIO BLANCO,[2] and HONG LI[1,2]

[1]Institute of Molecular Biophysics, Florida State University, Tallahassee, Florida 32306, USA
[2]Department of Chemistry and Biochemistry, Florida State University, Tallahassee, Florida 32306, USA

## ABSTRACT

**The structural basis for accurate placement of substrate RNA by H/ACA proteins is studied using a nonintrusive fluorescence assay. A model substrate RNA containing 2-aminopurine immediately 3′ of the uridine targeted for modification produces distinct fluorescence signals that report the substrate's docking status within the enzyme active site. We combined substrate RNA with complete and subcomplexes of H/ACA ribonucleoprotein particles and monitored changes in the substrate conformation. Our results show that each of the three accessory proteins, as well as an active site residue, have distinct effects on substrate conformations, presumably as docking occurs. Interestingly, in some cases these effects are exerted far from the active site. Application of our data to an available structural model of the holoenzyme, enables the functional role of each accessory protein in substrate placement to come into view.**

**Keywords: box H/ACA RNP; fluorescence assay; RNA conformational change; pseudouridylation**

## INTRODUCTION

H/ACA small nucleolar ribonucleoprotein particles (snoRNPs) and their archaeal homologs (sRNPs) are enzymes required for maturation of ribosomal RNA (rRNA) and small nuclear RNA (snRNA). A vast majority of H/ACA RNPs catalyze site-specific conversion of uridine to its C-glycosyl isomer, pseudouridine. In the modification process, H/ACA RNPs employ small noncoding RNAs to guide substrate RNA recognition and four proteins for pseudouridylation (Bortolin et al. 1999; Decatur and Fournier 2003; Meier 2006; Terns and Terns 2006). The guide RNA components of H/ACA sRNPs empower them to act on a large number of complicated RNA target sites that would otherwise require numerous protein enzymes of diverse specificities. On the other hand, the RNA-guided and multicomponent H/ACA RNPs face unusual challenges in binding and releasing these complicated RNA substrates (Weinstein and Steitz 1999; Fatica and Tollervey 2002; Hage and Tollervey 2004; Li 2008). The molecular mechanisms of how H/ACA RNPs meet these challenges remain unknown.

**Reprint requests to:** Hong Li, Institute of Molecular Biophysics, Florida State University, Tallahassee, FL 32306, USA; e-mail: hongli@sb.fsu.edu; fax: 850-644-7244.

Article published online ahead of print. Article and publication date are at http://www.rnajournal.org/cgi/doi/10.1261/rna.1109808.

A functional archaeal H/ACA RNP comprises an H/ACA guide RNA and four proteins: Cbf5 (rodent NAP57 and human dyskerin), L7Ae (yeast Nhp2p), Nop10, and Gar1 (Bousquet-Antonelli et al. 1997; Henras et al. 1998; Lafontaine et al. 1998; Dragon et al. 2000). RNA sequence analysis suggests that substrate RNAs bind to H/ACA RNPs primarily through base-pairing interactions with the H/ACA guide RNA. H/ACA RNAs are, typically, 70–250 nucleotides (nt) in lengths and contain a signature trinucleotide ACA at the 3′-end. Depending on the organism, the central portion of an H/ACA guide RNA contains at least one, or two, and occasionally three, helix–internal loop–helix hairpin units. The internal loop of each hairpin unit shares base complementarity between 8 and 16 bases with a substrate RNA (Fig. 1A). The unusual pairing between the substrate and the guide RNA creates a unique three-way junction that places the target uridine and the nucleotide 3′ to it at the center of the RNA duplex accessed by proteins (Fig. 1A). Structures of two such three-way junctions were recently observed in absence of proteins (Jin et al. 2007; Wu and Feigon 2007), thereby confirming the predicted secondary structure and moderate stability of the guide–substrate interactions.

Recent structural studies on archaeal H/ACA RNPs (Hamma et al. 2005; Li and Ye 2006; Manival et al. 2006; Rashid et al. 2006; Liang et al. 2007) and complementary biochemical studies (Wang and Meier 2004; Baker et al.

 

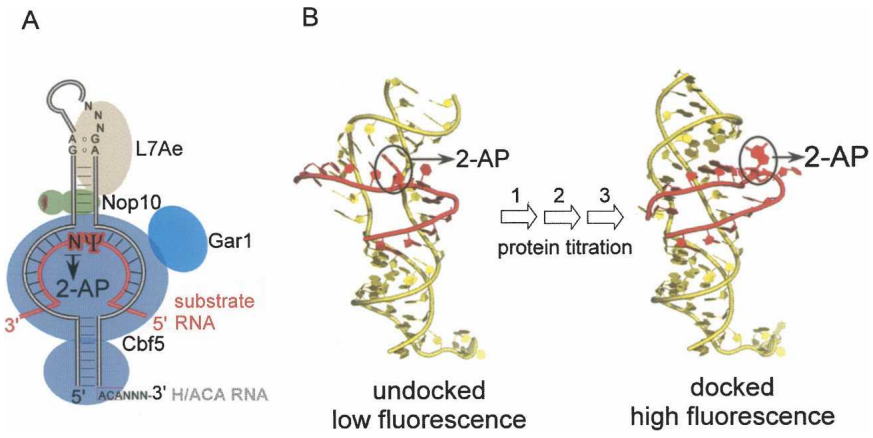


**FIGURE 1.** Schematic H/ACA RNP assembly and placement of a fluorescence label on the substrate RNA. (*A*) Composition and organization of box H/ACA RNPs. "Ψ" denotes the target uridine, which is to be converted to pseudouridine, and it is replaced by 5-floururidine (5-FU) unless noted otherwise. "N" denotes the nucleotide 3′ to the target uridine that is replaced by 2-aminopurine (2-AP). (*B*) An illustration of proposed changes in fluorescence intensities due to the conformation of the substrate RNA. The position of 2-AP is indicated. Docking of the substrate RNA leads to unstacking of 2-AP, thereby, high fluorescence intensity.

2005; Charpentier et al. 2005) suggest that H/ACA RNP proteins also play critical, although uncharacterized, roles in substrate RNA placement. Crystal structures of several substrate-free H/ACA RNPs revealed the three-dimensional network among the enzymatic components and led to the construction of a model of H/ACA RNP holoenzyme (Fig. 1A; Li and Ye 2006; Rashid et al. 2006). This model addresses parts of the mechanism of enzyme assembly while also raising several questions regarding how the accessory proteins participate in the modification process. Cbf5 is the catalytic subunit and the principal organizer of the entire RNP. Its role in substrate RNA placement is predicted to be through direct contacts with the substrate RNA, especially with the target uridine. Strikingly, however, Nop10, Gar1, and L7Ae (and presumably its eukaryotic homolog, Nh2p) (Wang and Meier 2004) are all placed more than 20 Å away from the catalytic site and far from the predicted binding tract of the substrate RNA, whereas biochemical assays have demonstrated essential roles of the three proteins in in vitro pseudouridylation assays (Wang and Meier 2004; Baker et al. 2005; Charpentier et al. 2005). Analysis of the only structure containing a substrate-bound H/ACA RNP without L7Ae suggests that L7Ae facilitates pseudouridylation from a long distance by placing the substrate within the active site (Liang et al. 2007). Similar mechanisms are believed to apply to Nop10 and Gar1 as well.

We previously devised a fluorescence assay based on 2-aminopurine (2-AP) which reported the conformation of the substrate RNA (Liang et al. 2007). We have systematically assessed the effect of each H/ACA RNP protein on 2-AP fluorescence and report here the profound effects they produce. The molecular basis underlying the functional roles of each H/ACA RNP protein is proposed based on the known structural data.

## RESULTS

### The 2-AP fluorescence assay

We substituted the nucleotide immediately 3′ to the substrate's target uridine by 2-aminopurine (2-AP) (Fig. 1B). The quantum yield of 2-AP is sensitive to its environment and exhibits strong quenching when AP is stacked (Rachofsky et al. 2001; Serrano-Andres et al. 2006). Thus, 2-AP has been extensively used to probe dynamics and kinetics of DNA–enzyme and RNA–enzyme interactions (Holz et al. 1998; Stivers 1998; Lenz et al. 2007). The identity of this nucleotide is not conserved, and its substitution by 2-AP is expected to have minimal impact on substrate binding and pseudouridylation activities. Therefore, substituted substrate conformations are expected to closely mimic those of the wild-type RNA substrate. Previous structural studies on substrate RNA binding (Liang et al. 2007) predict that the 2-AP nucleotide undergoes unstacking during substrate RNA docking into the active site (Fig. 1B). In addition to 2-AP, we also substituted the target uridine by 5-fluorouridine (5-FU), which is known to prevent pseudouridylation by forming 5-fluoro-6-hydroxpseudouridine (5FhΨ) (Hoang and Ferré-D'Amaré 2001; Spedaliere et al. 2004).

The 2-AP and 5-FU-substituted substrate RNA itself emits a low fluorescence signal (Fig. 2A). The substrate RNA annealed with guide RNA at 1:1 molar ratio did not induce a change in fluorescence signal. When a Cbf5–Nop10–Gar1 (CNG) complex or L7Ae alone was added separately to the annealed substrate–guide RNA complex, both reactions produced low level fluorescence intensity changes of <5% (Fig. 2A). These data indicate that the H/ACA RNP components used in assembly studies contribute only minimal background and that individual components do not cause significant changes in substrate RNA conformation.

### L7Ae affixes the H/ACA guide RNA for substrate docking

After preassembling the 2-AP and 5-FU-labeled substrate RNA with guide RNA and the CNG complex (CNG RNP), we studied the effect of L7Ae on substrate RNA placement. A significant increase in fluorescence intensity was observed when L7Ae was added to the substrate-bound CNG RNP (Fig. 2A), while L7Ae itself did not cause a change in fluorescence signal (Fig. 2A). The changes in fluorescence

intensity indicate that the 2-AP became fully unstacked, presumably because the substrate RNA was docked into the active site by L7Ae. The distinct fluorescence states of the substrate RNA in the presence and absence of L7Ae are consistent with the critical role revealed by crystallographic (Liang et al. 2007) and biochemical studies (Baker et al. 2005; Charpentier et al. 2005), supporting that anchoring H/ACA guide RNA's upper stem by L7Ae is required for substrate docking into the active site.

The L7Ae-induced fluorescence intensity change was found to be sensitive to the active site environment. We preassembled substrate and the guide RNA with the CNG ternary complex containing a Cbf5 mutant where the catalytic aspartate 85 was changed to alanine (CmNG). Addition of L7Ae to the substrate-bound CmNG complex produced a significantly reduced maximum fluorescence intensity, reflecting a different stacking state of the 2-AP in the absence of the catalytic aspartate (Fig. 2B). Since the final fluorescence intensity reached may also be sensitive to the catalytic step of conversion from 5FU to 5FhΨ (Hoang and Ferré-D'Amaré 2001), we cannot eliminate the possibility that the lower intensity was also due to unreacted target uridine.

## Nop10 further stabilizes the H/ACA RNA for substrate RNA docking

Nop10's potential role in substrate docking is also indicated by monitoring the 2-AP fluorescence response to a single-site mutant of Nop10. Residues Arg34 interacts with H/ACA RNA's upper stem in the L7Ae-bound structure (Li and Ye 2006). We substituted Arg34 with alanine and copurified the Nop10 mutant with the wild-type Cbf5 and Gar1 proteins (CNmG). Titration of L7Ae to the substrate-bound CNmG complex yielded a significantly lower maximum fluorescence intensity than the wild-type RNP (Fig. 2C). Previously, Branlant's laboratory showed that Nop10 is required for substrate binding (Charpentier et al. 2005), and that mutation of a residue near Arg34 (His31) in Nop10 impaired Cbf5's ability to modify a substrate RNA (Muller et al. 2007). Our result using CNmG corroborates this result and, more importantly, links the specific Nop10–guide RNA interaction directly to the behavior of the substrate's 2-AP nucleotide and potentially also to substrate docking.

It is significant to note that a family of dyskeratosis congenita (DC) patients contains the R34A mutation in Nop10 (Walne et al. 2007). Given that this position is either arginine or lysine in all Nop10 proteins, our findings provide a connection between this DC mutation and the RNA modification mechanisms of H/ACA RNPs.

## Gar1 remodels substrate RNA

Gar1 produces the most intriguing fluorescence responses. In the absence of Gar1 and L7Ae, saturating amounts of the

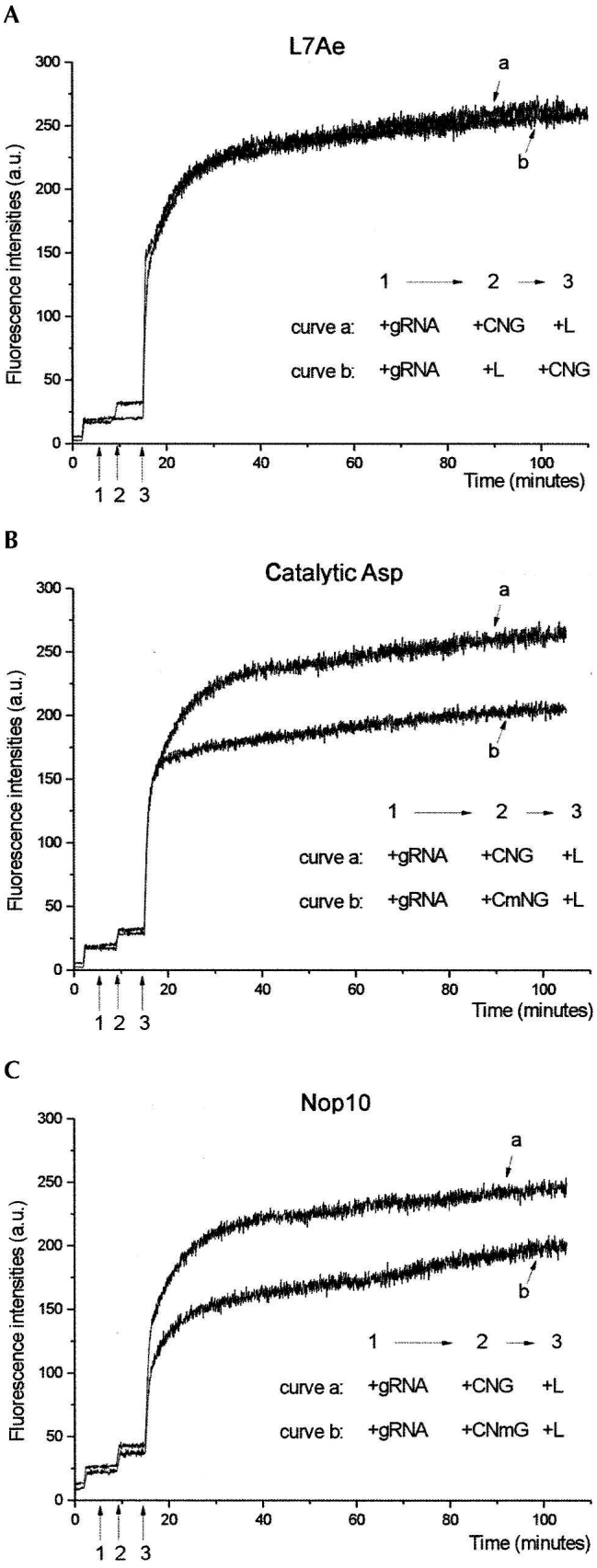


**FIGURE 2.** (Legend on next page)

Cbf5–Nop10 (CN) binary complex alone caused a surprisingly large increase in fluorescence intensity from the baseline (Fig. 3A). When 10-fold molar excess of Gar1 was subsequently titrated to the substrate-bound CN RNP, the fluorescence intensity decreased to almost baseline level (Fig. 3A). This observation suggests that without L7Ae, Gar1 potentially prohibits the substrate RNA from docking onto the active site. When the resulting CNG RNP subcomplex was titrated with saturating amounts of L7Ae, the fluorescence intensity rapidly increased to the same high level observed for the fully assembled RNP, suggesting that L7Ae overcomes the "inhibitory" effect of Gar1 (Fig. 3A).

When L7Ae was titrated before Gar1 into the substrate-bound CN complex, the 2-AP fluorescence reached a maximum value comparable to that observed for the fully assembled RNP, suggesting that L7Ae, Cbf5, and Nop10 alone can place the substrate RNA within the Cbf5 active site. In vitro activity studies showed that the CNL subcomplex is capable of modifying the substrate RNA, although less efficiently than the fully assembled RNP (Charpentier et al. 2005). Interestingly, titrating this resultant substrate-bound CNL subcomplex with saturating amounts of Gar1 caused a small reduction in the fluorescence intensity followed by a slow recovery to the full intensity (Fig. 3B). Reversing the titration order between L7Ae and the CN binary complex (data not shown) did not alter Gar1's effect on the substrate RNA. This observation suggests that Gar1 has the ability to remodel substrate RNA that is misdocked with partially assembled RNPs. This conformational effect by Gar1 may explain why Gar1 is not required for binding the guide RNA, yet it improves the efficiency of in vitro pseudouridylation activity (Charpentier et al. 2005).

The profound effect of Gar1 on the substrate RNA is in contrast to its long distance from the substrate. The distance between the nearest atoms of Gar1 and the substrate RNA is 20 Å. What, then, is the mechanism of Gar1's effect on substrate RNA? Of all the components in the H/ACA RNP, Gar1 interacts with Cbf5 exclusively. This interaction is primarily with Cbf5's conserved β7/β10 loop (Fig. 3E). Based on its similarity in location to TruB's RNA-binding thumb loop (Hoang and Ferré-D'Amaré 2001), the β7/β10 loop of Cbf5 was originally predicted to anchor the bound substrate RNA. We hypothesize that the β7/β10 loop mediates the Gar1's influence on substrate conformation. We shortened the β7/β10 loop of Cbf5 by deleting amino acids Ala148, Val149, and Lys150 (Δloop) and examined the resulting effect on Gar1's influence on the substrate. Where the wild-type RNP produced a small and recoverable dip in the substrate's fluorescence intensity, Gar1 titration to the substrate-bound C(Δloop)NL complex caused a larger and permanent drop in fluorescence intensity (Fig. 3C,D). While the β7/β10 loop alone is not sufficient to mediate remodeling of the substrate RNA by Gar1, it has a strong effect on the recovery phase following the initial drop in signal intensity (Fig. 3C,D). If the fluorescence recovery phase can be interpreted as substrate repositioning resulting in the 5FU conversion to 5FhΨ, Gar1 indeed plays a critical role in substrate placement via the β7/β10 loop of Cbf5.

**FIGURE 2.** The effects of L7Ae, catalytic aspartate, and Nop10 on substrate RNA docking. Fluorescence intensity at 363 nm was monitored while a substrate RNA labeled with both 2-AP and 5-FU and bound with guide RNA (gRNA), Cbf5, Nop10, and Gar1 (CNG RNP) was titrated with saturating amounts of L7Ae (*L*). Comparison of the fluorescence intensity profiles of L7Ae titration to the wild-type CNG RNP (*A*), L7Ae titration to the CGN RNP containing catalytic aspartate to alanine mutation (CmNG) (*B*), L7Ae titration to CNG RNP containing Nop10 Arg34 to alanine mutation (CNmG) (*C*). Labels "1," "2," and "3" indicate the order of titration steps of the specified subunits. Arrows indicate titration points.

## Conformational effects due to isomerization of uridine

We next addressed the question if the 2-AP fluorescence is sensitive to the chemical identity of the target uridine and specifically to the process of uridine isomerization (5-FU versus wild-type U). Results obtained with the 5-FU-labeled substrate RNA suggested that this is possible but did not yield a clear correlation between 2-AP fluorescence and chemical identity of the target uridine. This may be because the 5-FU-lableled substrate does not allow the enzyme to proceed to the last step of pseudouridylation. We therefore performed the fluorescence assay with a substrate labeled only with 2-AP without substitution of the target uridine. The effect of H/ACA RNP assembly on the wild-type substrate RNA is quite interesting, and may reflect the catalytic process. The substrate-bound CNL RNP showed an initially high fluorescence intensity followed by a slow and steady decay that was interrupted by addition of the fourth protein, Gar1 (Fig. 4A). The same final fluorescence intensity level could be reached regardless of when Gar1 was added (data not shown). We interpret the slow decay of the fluorescence as inefficient isomerization of the target uridine by the CNL complex. Addition of Gar1 accelerated this process and led to a rapid reduction of the fluorescence intensity. This interpretation is consistent with the known catalytic properties of the CNL and the full CNLG complex (Muller et al. 2007).

To confirm the cause for the fluorescence decay, we observed the effect of the catalytically deficient CmN complex on fluorescence intensity from the wild-type substrate. Similar to the wild-type CN complex, the CmN complex caused an initial increase in fluorescence intensity, though smaller in scale. Subsequent addition of L7Ae brought the fluorescence intensity a maximal level where, unlike the wild-type CNL complex, the signal remained high without further decay (Fig. 4B).

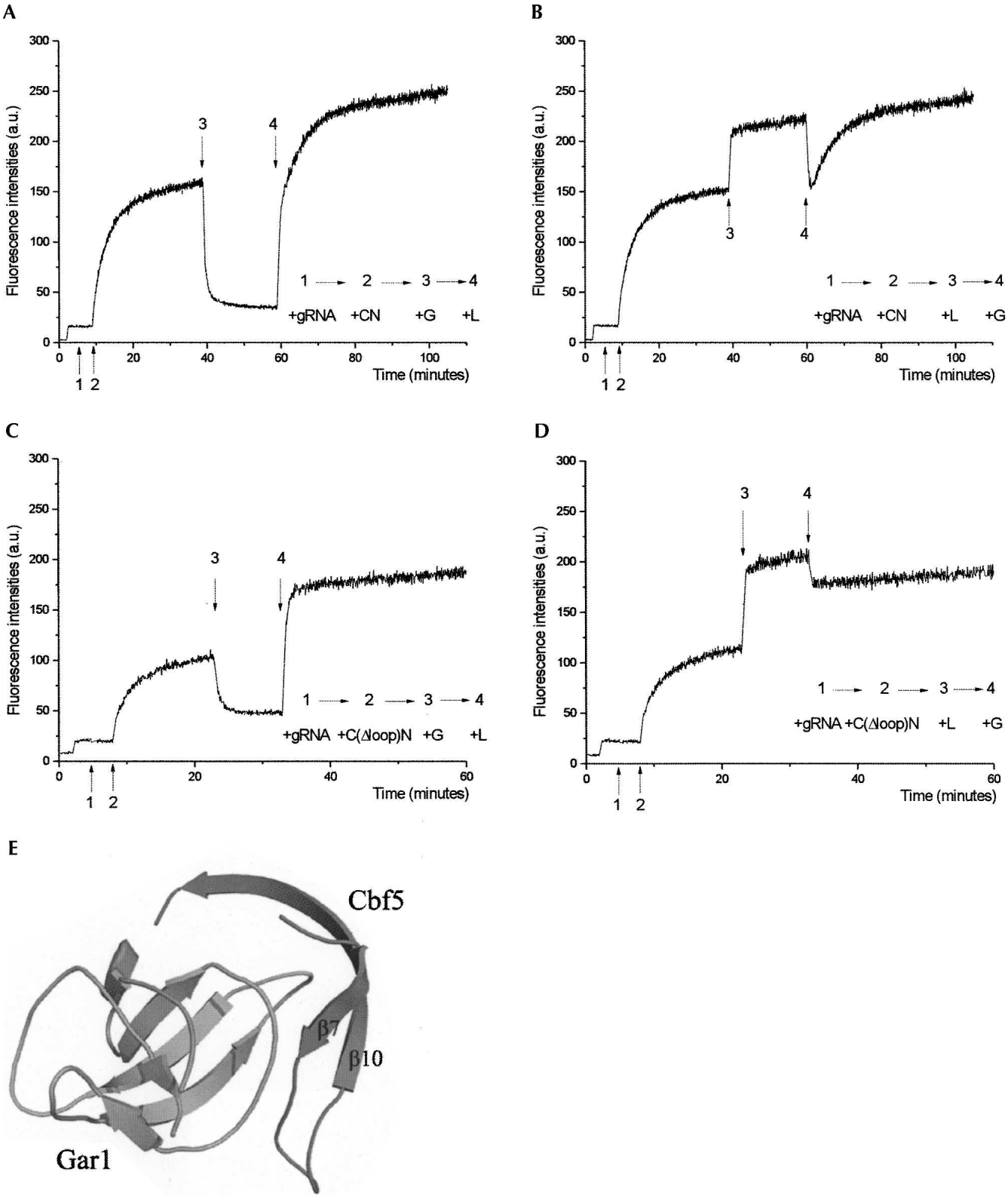


**FIGURE 3.** The effects of Gar1 on substrate RNA docking. (*A*) Fluorescence intensity profile of substrate RNA bound with guide RNA (gRNA),Cbf5, and Nop10 (CN RNP) when Gar1 was added before L7Ae. (*B*) Fluorescence intensity profile of substrate RNA bound with guide RNA,Cbf5, and Nop10 (CN RNP) when Gar1 was added after L7Ae.; (*C*) the same titration as of *A* but with Cbf5 Δloop mutation; (*D*) the same titration order as of *B* but with Cbf5 Δloop mutation. (*E*) Previously observed interactions between Gar1 and the β7/β10 loop of Cbf5. The coordinates are from crystal structure of the *P. furiosus* Cbf5–Nop10–Gar1 complex (PDB code 2EY4).

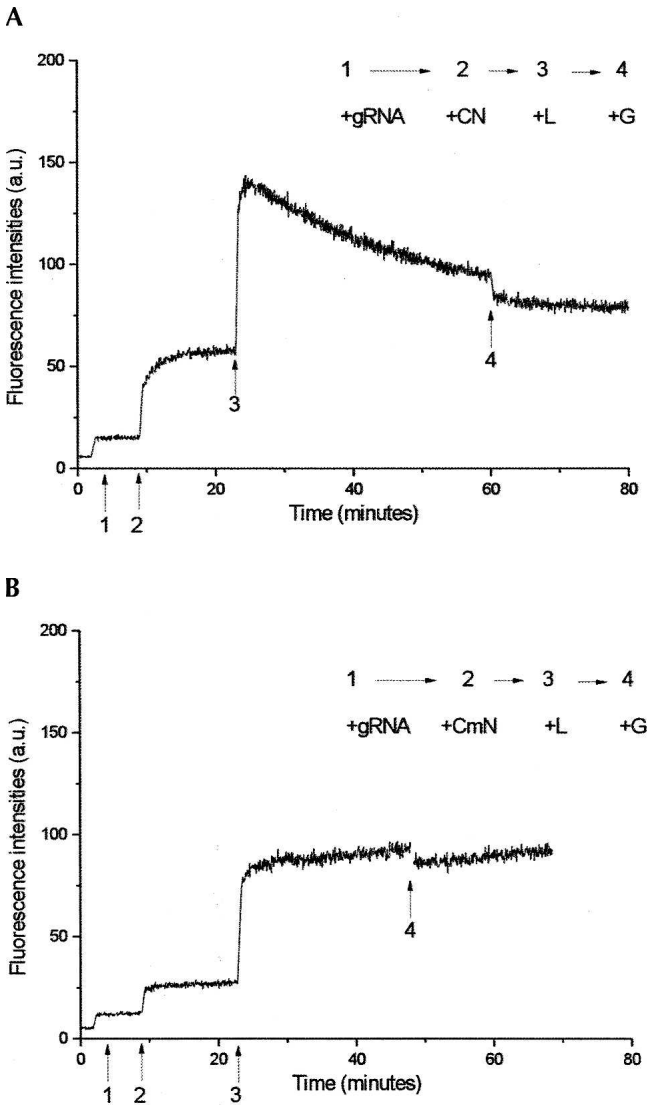


**FIGURE 4.** Conformational effects of the wild-type substrate RNA. The fluorescence profile of titrating a substrate labeled with 2-AP and unsubstituted target uridine with the wild-type H/ACA RNP (*A*) and the catalytically defficient H/ACA RNP (*B*).

### Thermodynamics of substrate binding suggests an efficient H/ACA RNP assembly pathway

To understand the energetic cost of moving the substrate RNA into H/ACA RNP's active site, we measured apparent binding constants of L7Ae and CNG complex. Since the fluorescence intensity is a measure of the amount of unstacked 2-AP in the substrate RNA, the apparent binding constant obtained by the 2-AP fluorescence assay most likely reflects the combined processes of ground-state guide RNA binding by each protein (or protein complex) and subsequent active site docking of the substrate RNA.

Nonlinear least-square fitting of an average fluorescence intensity dependence on L7Ae concentrations yielded an apparent dissociation constant of 18 ± 17 nM for L7Ae binding to the RNA substrate bound to the CNG RNP (Fig. 5A). This value is significantly greater than the dissociation constant of 0.7–5 nM for L7Ae binding to a K-turn RNA (Kuhn et al. 2002; Turner et al. 2005). Assuming a similar binding constant for the K-turn in our guide RNA by L7Ae, the additional energetic cost would arise from the step of substrate docking. Perhaps the pathway for substrate docking is not always open and thus many encounters between L7Ae and the substrate-bound CNG RNP do not result in docking of the substrate RNA.

Nonlinear least-square fit of an average fluorescence intensity dependence on CNG concentrations yielded an apparent dissociation constant of 41 ± 10 nM (Fig. 5B), a value significantly smaller than the estimated dissociation constant of Cbf5 for the guide RNA by gel mobility shift assay (~400 nM) (Baker et al. 2005). The additional proteins bound to the guide RNA and to Cbf5 likely account for the observed increase in affinity. Therefore, CNG docking following L7Ae binding produces an extremely efficient substrate placement process. This is in contrast to its relatively inefficient docking by L7Ae following CNG binding, and therefore suggests an H/ACA RNP assembly order favorable for substrate placement.

## DISCUSSION

While crystallographic data accumulate rapidly on H/ACA RNPs, it remains unclear how H/ACA RNPs accurately bind to substrate RNA. This is partly due to the absence of an efficient assay that monitors the complicated process of substrate RNA binding to H/ACA RNPs. We developed a fluorescence method by taking advantage of the structural homology with natural nucleotides and desirable fluorescence properties of 2-AP. A substrate RNA bearing 2-AP reports significant fluorescence intensity changes that indicate the likelihood of correct substrate docking into the enzyme active site. The fluorescence changes seen were found to be dependent on the coordinated actions of all four H/ACA RNP proteins, even at long distances (Fig. 6).

Our recent crystallographic study suggests that L7Ae affects catalysis through indirect placement of the substrate RNA. Comparing an L7Ae-free RNP structure (Liang et al. 2007) to that of an L7Ae-bound RNP (Li and Ye 2006) suggests that L7Ae positions the guide RNA by fastening its upper stem on the catalytic domain of Cbf5. The L7Ae-induced conformational change in the guide RNA was also observed by Terns's laboratory using an RNA footprinting method (Baker et al. 2008). The conformation of the guide RNA was predicted to influence that of the paired substrate RNA. Our fluorescence study confirms this proposed role of L7Ae. Similarly, these results support previous data on Nop10's effect on substrate placement. Nop10 is positioned along the linear track of the guide RNA and has essential roles in anchoring it (Li and Ye 2006; Muller et al. 2007). Like L7Ae, it places the substrate RNA indirectly via positioning the guide RNA upper stem.

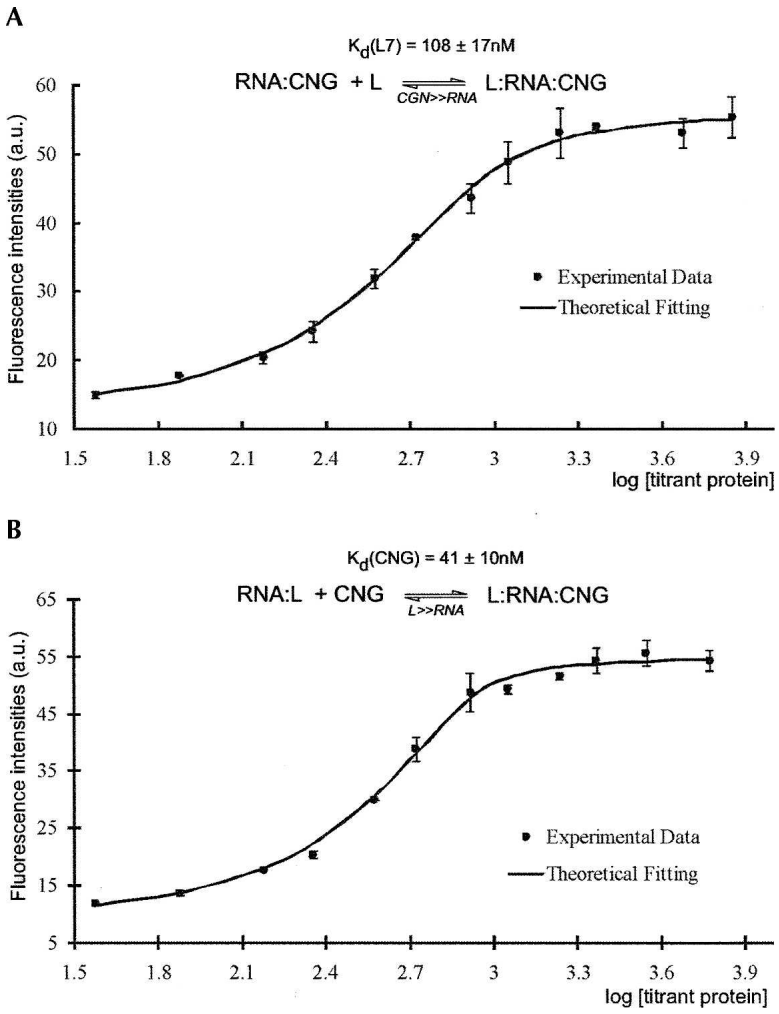


**FIGURE 5.** Thermodynamic parameters of substrate RNA docking. (*A*) The apparent dissociation constant of L7Ae, $K_d$ (L7), was obtained by monitoring florescence intensities as a function of L7Ae concentration followed by nonlinear least-square fitting. In the titration experiment, the CNG complex was in molar excess of the guide–substrate RNA complex. (*B*) The apparent dissociation constant of CNG, $K_d$ (CNG), was obtained by monitoring florescence intensities as a function of CNG concentration followed by nonlinear least-square fitting. In the titration experiment, L7Ae was in molar excess of the guide–substrate RNA complex.

The molecular basis for Gar1's potential role in substrate placement remains unclear. Like L7Ae and Nop10, Gar1 is far from both the active site and the predicted substrate binding site. Unlike L7Ae and Nop10, however, Gar1 has no direct contact with either the guide or the substrate RNA. Yet, Gar1 clearly influences the placement of substrate in an L7Ae-dependent manner. In the absence of L7Ae (but presence of CN), the substrate is completely prohibited from docking by Gar1. In the presence of L7Ae, where fluorescence indicates that substrate RNA is largely docked, Gar1 seemingly repositions the substrate RNA. It is known that Gar1 interacts with a well-conserved loop of Cbf5 (β7/β10 loop) which has been proposed to anchor the substrate RNA (Li and Ye 2006; Rashid et al. 2006). Our mutational studies show that shortening of the β7/β10 loop altered Gar1's effects on fluorescence to indicate the likelihood that Gar1's ability to remodel substrate RNA was abolished but Gar1 also retained its ability to prevent substrate from docking in the absence of L7Ae. These observations suggest that both the globular domain and the β7/β10 loop of Cbf5 are required for mediating Gar1's action.

Gar1 is also known to be essential for the processing function of H/ACA RNP (Girard et al. 1992). In yeast, Gar1 is found to be associated with the processing H/ACA RNAs snR10 and snR30 (U17 human) and its deletion accumulates unprocessed 18S (Girard et al. 1992) RNA. The fact that snR30 RNA uses the central internal loop (equivalent to the Ψ pocket) for the essential guiding function (Atzorn et al. 2004) suggests the possibility that Gar1's conformational effects illustrated here also have a role in rRNA processing.

The mammalian Gar1 is known to the be last protein bound to the RNP by exchanging with assembly factor Naf1 (Darzacq et al. 2006; Leulliot et al. 2007). If the role of archaeal Gar1 can be extrapolated to mammalian Gar1, our discovery that Gar1 remodels the substrate provides an explanation for the temporal order of Gar1. The dynamic exchange between Naf1 and Gar1 can serve to control the timing of RNA modification.

The thermodynamic data on substrate RNA placement suggest a preferred order of assembly between L7Ae and the CNG complex. First, the dissociation constant between L7Ae and the substrate bound CNG RNP, is significantly higher than the well-documented low dissociation constant between L7Ae and kink-turn RNA (Kuhn et al. 2002; Turner et al. 2005). This may be interpreted as the existence of docking obstacles along the path of substrate placement by L7Ae in the CNG RNP. In contrast, the dissociation constant between the CNG ternary complex and the substrate bound to L7Ae RNP is low. Considering the known high binding energy of Cbf5 to L7Ae-free guide RNA (Baker et al. 2005) but low binding energy of L7Ae to Cbf5-free guide RNA, these new thermodynamic data favor an assembly model in which L7Ae binds to guide RNA first followed by Cbf5 or the CNG complex. This model of archaeal H/ACA RNP assembly may apply to the mammalian system with certain modifications. The mammalian homolog of L7Ae, NH2P,

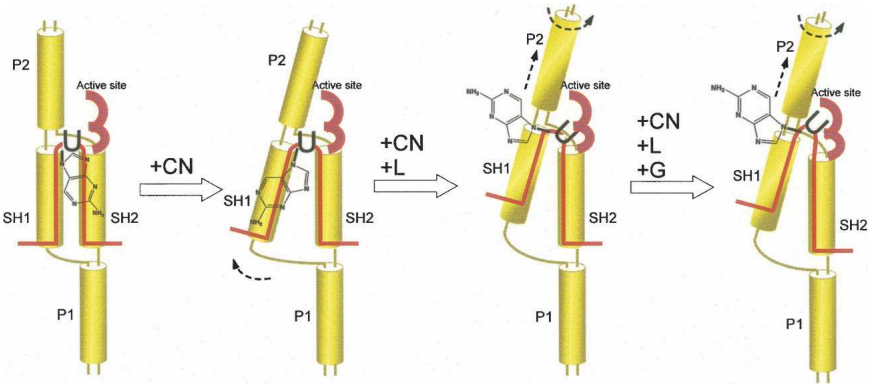


**FIGURE 6.** Distinct substrate RNA conformations in partially and fully docked complexes are revealed by fluorescence studies. A cartoon representation of substrate conformations accounting for the observed fluorescence intensities. "U" denotes the target uridine and the fused rings represent 2-AP. Yellow cylinders represent the four helices formed by the guide–substrate RNA complex.

is known to form a protein complex with the NAP57–NOP10 binary complex before association with RNA (Wang and Meier 2004). Therefore, the mammalian particle assembles the NAP57–NOP10–NH2P trimer proteins in a single step.

The precursor rRNA must be released by H/ACA RNPs after modification to allow assembly of the ribosome. However, the mechanism of release remains unexplored. Does modified uridine signal changes in enzyme conformation that ultimately lead to release of the product? Are exogenous factors such as ATPases required for disruption of substrate-H/ACA RNP interactions? Although a number of ATPases have been reported to facilitate rRNA processing H/ACA RNPs (Venema et al. 1997; Kos and Tollervey 2005; Liang and Fournier 2006), it is difficult to imagine how ATPases, if involved in product release, distinguish unmodified from modified RNA. Our results suggest that the substrate conformation is sensitive to the chemical identity of the target uridine. This can be a potential molecular basis for product release either with or without the requirement for ATPases.

## MATERIALS AND METHODS

Production of protein samples was done as described previously (Rashid et al. 2006). 2-AP and 5-FU-labeled substrates were purchased from Dharmacon (Thermo Fisher Scientific, Inc.). All fluorescence experiments were carried out on a Cary Eclipse fluorescence spectrophotometer (Varian, Inc.) at 50°C. In general, to monitor the effect of each H/ACA RNP protein on 2-AP fluorescence, we preassembled subcomplexes in a binding buffer containing 300 mM NaCl, 25 mM $MgCl_2$, and 180 mM Na Citrate. To observe the effect of a particular protein or protein complex, saturating amounts of the protein were added to the preassembled complex and the fluorescence intensity was followed in kinetics mode until a plateau was reached. We used an excitation wavelength 325 nm and the emission wavelength 363 nm, where minimal protein absorbance and fluorescence were observed. The concentration of substrate RNA was 1.20 μM. The molar ratio of a typical preassembled RNP subcomplex is 1:1:10 for substrate RNA:guide RNA:protein(s). The subsequent titrant protein or protein complex is also 10-fold molar excess of the substrate RNA.

The titration experiments were assembled by step-wise addition of a protein to a preassembled RNP subcomplex with a total increase in volume <1%. Since L7Ae does not interact with the CNG complex, the change in fluorescence intensity versus titrant protein concentration reports the isotherm of titrant protein binding to guide RNA followed by substrate remodeling. The inner filter effect was also ruled out because H/ACA proteins do not have significant absorption at the excitation wavelength (data not shown). The model was based on the typical enzyme (E) and substrate (S) binding system: $E + S \Leftrightarrow ES$, and the fluorescence intensity is assumed to be a linear proportion of substrate RNA in the bound state compared to total substrate RNA present. The apparent dissociation constant $K_d$ was determined by least-square fitting the fluorescence intensity ($F$) of the 2-AP using equation 1, where $[E_{total}]$ is the total enzyme concentration, $[S_{total}]$ is the total substrate concentration, and $F_0$ and $F_{max}$ are the fluorescence intensities at zero and saturating concentrations of titrant protein, respectively.

$$F = F_0 + (F_{max} - F_0) \times \frac{([E_{total}]+[S_{total}]+K_d) - \sqrt{([E_{total}]+[S_{total}]+K_d)^2 - 4[E_{total}][S_{total}]}}{2[E_{total}]}. \quad (1)$$

The sample was generally incubated for 12–15 min to allow equilibrium to be reached before any measurements were taken. Each data point in the curve was the average for at least five repeated scans and the reported dissociation constants were averaged from the independent titration experiments.

## ACKNOWLEDGMENTS

This work was supported by NIH grant R01 GM66958-01. B.L. is a predoctoral fellow of American Heart Association, Florida/Puerto Rico Affiliate (0615182B). K.C. is an American Heart Association Florida/Puerto Rico Affiliate predoctoral fellow (0415091B). We thank Dr. Dongping Zhong for advice on the 2-AP fluorescence.

*Received March 31, 2008; accepted June 12, 2008.*

## REFERENCES

Atzorn, V., Fragapane, P., and Kiss, T. 2004. U17/snR30 is a ubiquitous snoRNA with two conserved sequence motifs essential for 18S rRNA production. *Mol. Cell. Biol.* **24:** 1769–1778.

Baker, D.L., Youssef, O.A., Chastkofsky, M.I., Dy, D.A., Terns, R.M., and Terns, M.P. 2005. RNA-guided RNA modification: Functional

organization of the archaeal H/ACA RNP. *Genes & Dev.* **19:** 1238–1248.

Baker, D.L., Seyfried, N.T., Li, H., Orlando, R., Terns, R.M., and Terns, M.P. 2008. Determination of protein–RNA interaction sites in the Cbf5-H/ACA guide RNA complex by mass spectrometric protein footprinting. *Biochemistry* **47:** 1500–1510.

Bortolin, M.L., Ganot, P., and Kiss, T. 1999. Elements essential for accumulation and function of small nucleolar RNAs directing site-specific pseudouridylation of ribosomal RNAs. *EMBO J.* **18:** 457–469.

Bousquet-Antonelli, C., Henry, Y., G'Elugne, J.P., Caizergues-Ferrer, M., and Kiss, T. 1997. A small nucleolar RNP protein is required for pseudouridylation of eukaryotic ribosomal RNAs. *EMBO J.* **16:** 4770–4776.

Charpentier, B., Muller, S., and Branlant, C. 2005. Reconstitution of archaeal H/ACA small ribonucleoprotein complexes active in pseudouridylation. *Nucleic Acids Res.* **33:** 3133–3144.

Darzacq, X., Kittur, N., Roy, S., Shav-Tal, Y., Singer, R.H., and Meier, U.T. 2006. Stepwise RNP assembly at the site of H/ACA RNA transcription in human cells. *J. Cell Biol.* **173:** 207–218.

Decatur, W.A. and Fournier, M.J. 2003. RNA-guided nucleotide modification of ribosomal and other RNAs. *J. Biol. Chem.* **278:** 695–698.

Dragon, F., Pogacic, V., and Filipowicz, W. 2000. In vitro assembly of human H/ACA small nucleolar RNPs reveals unique features of U17 and telomerase RNAs. *Mol. Cell. Biol.* **20:** 3037–3048.

Fatica, A. and Tollervey, D. 2002. Making ribosomes. *Curr. Opin. Cell Biol.* **14:** 313–318.

Girard, J.P., Lehtonen, H., Caizergues-Ferrer, M., Amalric, F., Tollervey, D., and Lapeyre, B. 1992. GAR1 is an essential small nucleolar RNP protein required for pre-rRNA processing in yeast. *EMBO J.* **11:** 673–682.

Hage, A.E. and Tollervey, D. 2004. A surfeit of factors: Why is ribosome assembly so much more complicated in eukaryotes than bacteria? *RNA Biol.* **1:** 10–15.

Hamma, T., Reichow, S.L., Varani, G., and Ferre-D'Amare, A.R. 2005. The Cbf5–Nop10 complex is a molecular bracket that organizes box H/ACA RNPs. *Nat. Stuct. Mol. Biol.* **12:** 1101–1107.

Henras, A., Henry, Y., Bousquet-Antonelli, C., Noaillac-Depeyre, J., Gelugne, J.P., and Caizergues-Ferrer, M. 1998. Nhp2p and Nop10p are essential for the function of H/ACA snoRNPs. *EMBO J.* **17:** 7078–7090.

Hoang, C. and Ferré-D'Amaré, A.R. 2001. Cocrystal structure of a tRNA Psi55 pseudouridine synthase: Nucleotide flipping by an RNA-modifying enzyme. *Cell* **107:** 929–939.

Holz, B., Klimasauskas, S., Serva, S., and Weinhold, E. 1998. 2-Aminopurine as a fluorescent probe for DNA base flipping by methyltransferases. *Nucleic Acids Res.* **26:** 1076–1083.

Jin, H., Loria, J.P., and Moore, P.B. 2007. Solution structure of an rRNA substrate bound to the pseudouridylation pocket of a box H/ACA snoRNA. *Mol. Cell* **26:** 205–215.

Kos, M. and Tollervey, D. 2005. The putative RNA helicase Dbp4p is required for release of the U14 snoRNA from preribosomes in *Saccharomyces cerevisiae*. *Mol. Cell* **20:** 53–64.

Kuhn, J.F., Tran, E.J., and Maxwell, E.S. 2002. Archaeal ribosomal protein L7 is a functional homolog of the eukaryotic 15.5kD/Snu13p snoRNP core protein. *Nucleic Acids Res.* **30:** 931–941.

Lafontaine, D., Bousquet, A.C., Henry, Y., Caizergues, F.M., and Tollervey, D. 1998. The box H + ACA snoRNAs carry Cbf5p, the putative rRNA pseudouridine synthase. *Genes & Dev.* **12:** 527–537.

Lenz, T., Bonnist, E.Y., Pljevaljcic, G., Neely, R.K., Dryden, D.T., Scheidig, A.J., Jones, A.C., and Weinhold, E. 2007. 2-Aminopurine flipped into the active site of the adenine-specific DNA methyltransferase M.TaqI: Crystal structures and time-resolved fluorescence. *J. Am. Chem. Soc.* **129:** 6240–6248.

Leulliot, N., Godin, K.S., Hoareau-Aveilla, C., Quevillon-Cheruel, S., Varani, G., Henry, Y., and Van Tilbeurgh, H. 2007. The box H/ACA RNP assembly factor Naf1p contains a domain homologous to Gar1p mediating its interaction with Cbf5p. *J. Mol. Biol.* **371:** 1338–1353.

Li, H. 2008. Unveiling substrate RNA binding to H/ACA RNPs: One side fits all. *Curr. Opin. Struct. Biol.* **18:** 78–85.

Li, L. and Ye, K. 2006. Crystal structure of an H/ACA box ribonucleoprotein particle. *Nature* **443:** 302–307.

Liang, B., Xue, S., Terns, R.M., Terns, M.P., and Li, H. 2007. Substrate RNA positioning in the archaeal H/ACA ribonucleoprotein complex. *Nat. Struct. Mol. Biol.* **14:** 1189–1195.

Liang, X.H. and Fournier, M.J. 2006. The helicase Has1p is required for snoRNA release from pre-rRNA. *Mol. Cell. Biol.* **26:** 7437–7450.

Manival, X., Charron, C., Fourmann, J.B., Godard, F., Charpentier, B., and Branlant, C. 2006. Crystal structure determination and site-directed mutagenesis of the *Pyrococcus abyssi* aCBF5-aNOP10 complex reveal crucial roles of the C-terminal domains of both proteins in H/ACA sRNP activity. *Nucleic Acids Res.* **34:** 826–839.

Meier, U.T. 2006. How a single protein complex accommodates many different H/ACA RNAs. *Trends Biochem. Sci.* **31:** 311–315.

Muller, S., Fourmann, J.B., Loegler, C., Charpentier, B., and Branlant, C. 2007. Identification of determinants in the protein partners aCBF5 and aNOP10 necessary for the tRNA:Psi55-synthase and RNA-guided RNA:Psi-synthase activities. *Nucleic Acids Res.* **35:** 5610–5624.

Rachofsky, E.L., Osman, R., and Ross, J.B. 2001. Probing structure and dynamics of DNA with 2-aminopurine: Effects of local environment on fluorescence. *Biochemistry* **40:** 946–956.

Rashid, R., Liang, B., Baker, D.L., Youssef, O.A., He, Y., Phipps, K., Terns, R.M., Terns, M.P., and Li, H. 2006. Crystal structure of a Cbf5–Nop10–Gar1 complex and implications in RNA-guided pseudouridylation and dyskeratosis congenita. *Mol. Cell* **21:** 249–260.

Serrano-Andres, L., Merchan, M., and Borin, A.C. 2006. Adenine and 2-aminopurine: paradigms of modern theoretical photochemistry. *Proc. Natl. Acad. Sci.* **103:** 8691–8696.

Spedaliere, C.J., Ginter, J.M., Johnston, M.V., and Mueller, E.G. 2004. The pseudouridine synthases: Revisiting a mechanism that seemed settled. *J. Am. Chem. Soc.* **126:** 12758–12759.

Stivers, J.T. 1998. 2-Aminopurine fluorescence studies of base stacking interactions at abasic sites in DNA: Metal-ion and base sequence effects. *Nucleic Acids Res.* **26:** 3837–3844.

Terns, M. and Terns, R. 2006. Noncoding RNAs of the H/ACA Family. *Cold Spring Harb. Symp. Quant. Biol.* **71:** 395–405.

Turner, B., Melcher, S.E., Wilson, T.J., Norman, D.G., and Lilley, D.M. 2005. Induced fit of RNA on binding the L7Ae protein to the kink-turn motif. *RNA* **11:** 1192–1200.

Venema, J., Bousquet-Antonelli, C., Gelugne, J.P., Caizergues-Ferrer, M., and Tollervey, D. 1997. Rok1p is a putative RNA helicase required for rRNA processing. *Mol. Cell. Biol.* **17:** 3398–3407.

Walne, A.J., Vulliamy, T., Marrone, A., Beswick, R., Kirwan, M., Masunari, Y., Al-Qurashi, F.H., Aljurf, M., and Dokal, I. 2007. Genetic heterogeneity in autosomal recessive dyskeratosis congenita with one subtype due to mutations in the telomerase-associated protein NOP10. *Hum. Mol. Genet.* **16:** 1619–1629.

Wang, C. and Meier, U.T. 2004. Architecture and assembly of mammalian H/ACA small nucleolar and telomerase ribonucleoproteins. *EMBO J.* **23:** 1857–1867.

Weinstein, L.B. and Steitz, J.A. 1999. Guided tours: From precursor snoRNA to functional snoRNP. *Curr. Opin. Cell Biol.* **11:** 378–384.

Wu, H. and Feigon, J. 2007. H/ACA small nucleolar RNA pseudouridylation pockets bind substrate RNA to form three-way junctions that position the target U for modification. *Proc. Natl. Acad. Sci.* **104:** 6655–6660.